Performance improvement of solar-assisted air-conditioning systems by using an innovative configuration of a desiccant dehumidifier and thermal recovery unit

Mohamed Abdelgaied[1] · Mohamed A. Saber[1] · M. M. Bassuoni[1] · Ahmad M. Khaira[1]

Abstract

The present study aims to construct an innovative configuration of a desiccant air conditioner that achieves thermal comfort conditions with the lowest electrical power consumption rates. To achieve this, an innovative configuration of a desiccant dehumidifier channel with multi-stages of silica-gel pads and heat exchangers for inter-cooling (DDC-MSSGP&HEI) was incorporated with the suggested air conditioner. The DDC-MSSGP&HEI is characterized by increasing the dehumidification capacity as well as cooling the process air with cooling rates higher than the heat generated by the adsorption heat effect. The thermal recovery unit was also incorporated with the suggested air conditioner to achieve the lowest electrical power consumption rates; it was utilized as a preheating unit to heat the regeneration air before entering into the solar collectors. The results showed that the system could supply air with a temperature of 12.2 °C and a humidity ratio of 7 g_w kg_{da}^{-1}, this is because of the positive effect of DDC-MSSGP&HEI. Also, the energy performance of the innovative configuration of a desiccant air conditioner is more efficient where TCOP and ECOP reached 1.96 and 3.14, respectively at a regeneration temperature of 90 °C. Moreover, the energy saving due to the utilization of the thermal recovery unit reached 28.7%. The economic feasibility indicates that the proposed configuration has the potential to save the life cycle cost by a rate of up to 33% compared to the conventional system with a payback period of 5.8 years.

Keywords Air conditioner · Innovative configuration of desiccant dehumidifier · Silica-gel pads with intercooling · Solar energy · Thermal recovery unit · Performance improvement

Abbreviations

AEAH	Auxiliary electrical air heater
BFCV	Butterfly control valves
CFPHE	Counter flow plate heat exchanger
DDC-MSSGP&HEI	Desiccant dehumidifier channel with multi-stages of silica-gel pads and heat exchangers for intercooling
DEC	Direct evaporative cooler
DPASC	Double path air solar collector
ETWSC	Evacuated tube water solar collector
ETWSCHE	Evacuated tube water solar collectors heat exchanger
HDH	Humidification dehumidification unit
PCM	Phase change material
OTSDC	One-rotor two-stage rotary desiccant cooling
TSDC	Two-stage desiccant cooling
C_p	Specific heat capacity, kJ kg^{-1} K^{-1}
DCOP	Dehumidification coefficient of performance,
DC	Dehumidification capacity, g_w kg_{da}^{-1}
d	Discount rate
ECOP	Electrical coefficient of performance
h	Air specific enthalpy, kJ kg^{-1}
h_{fg}	Latent heat of water vaporization, kJ kg^{-1}
i	Interest rate
IC	Initial cost, $
LCC	Life cycle cost, $
$\dot{m}$	Air mass flow rate, kg s^{-1}

✉ Mohamed Abdelgaied
   mohamed_abdelgaied@f-eng.tanta.edu.eg

1 Mechanical Power Engineering Department, Faculty of Engineering, Tanta University, Tanta, Egypt

Springer

MRC	Moisture removal capacity, $g_w\ s^{-1}$
N	Life cycle, year
OC	Operating cost, \$
P_{fans}	Fan power, kW
P_{pumps}	Pump power, kW
PP	Payback period, year
PWF	Present worth factor, -
$\dot{Q}_c$	Refrigeration capacity, kW
$\dot{Q}_{th,AEAH}$	Rate of heat transfer to regeneration air in AEAH, kW
$\dot{Q}_{th,DPSAC}$	Rate of heat transfer to regeneration air in DPSAC, kW
$\dot{Q}_{th,ETWSC}$	Rate of heat transfer to regeneration air in ETWSC, kW
SF	Solar fraction, -
TCOP	Thermal coefficient of performance, -
T	Temperature, ^oC
ω	Humidity ratio, $g_w\ kg_{da}^{-1}$

Subscript

p	Process air
reg	Regeneration air

Introduction

As a result of directions to rationalize power consumption and protect the environment from harmful emissions, the world began to reduce the use of traditional air conditioning systems and replace it with desiccant air conditioning systems which overcome the traditional systems' problems of consuming a large amount of electrical power and emissions of chlorofluorocarbons gases that harm the environment and leads to increase the ambient air temperature. Also, the desiccant air conditioner systems can handle latent/sensible loads separately compared to traditional air conditioner systems and can be regenerated using renewable energy and low-grade heat energy. The basic idea of the desiccant air conditioner is to integrate desiccant dehumidification technologies, heat exchangers, and evaporative coolers. A desiccant air conditioner can classify into two categories liquid desiccant air conditioner and solid desiccant air conditioner which consist of a rotary wheel as the main part. All these technologies are widely used because of their advantages, especially the rotary desiccant air conditioning systems. To date, many studies have been performed to predict the performance of rotary desiccant air conditioners on basis of mathematical simulation [1, 2], an experimental investigation [3–5], thermodynamic analysis [6], and practical application [7–9]. The first rotary desiccant air conditioner which is called the Pennington cycle or ventilation cycle was introduced by Pennington in 1955 [10]. To increase cooling

capacity and coefficient of performance, return air is used as process air resulting in a recirculation cycle. In another way to increase the cooling capacity, Dunkle [11] added an extra heat exchanger in the recirculation cycle that can provide colder process air to the main heat exchanger. Multi-stage cycles are also proposed to compact the adsorption heat effect and increase system performance. According to this, two types of two-stage systems are introduced by Ge et al. [3, 4], one is two-stage desiccant cooling (TSDC) system based on two rotary desiccants and the other is one-rotor two-stage desiccant cooling (OTSDC) using one wheel. The division of the cross-section of the wheel is the main difference between the two cycles. A desiccant wheel of TSDC is divided into two sections: each for regeneration and the other for a process like a conventional desiccant wheel while the OTSDC wheel is divided into four sections: two sections for regeneration and two sections for the process. Composite silica gel-lithium chloride has been utilized in two systems and internal coolers have been incorporated to increase the system performance. The results confirmed that the two systems can operate with energy sources above 50 °C and get a coefficient of performance over 1.0. For the TSDC system, the required regeneration temperature is decreased from 100 to 70 °C at moisture removal of 6 $g_w\ kg_{da}^{-1}$ compared with traditional one-stage under ARI summer conditions. Note that, the size of OTSDC is about half of TSDC which makes it suitable for residential buildings. Elzahzby et al. [12] introduced a one-rotor six-stage desiccant system whose wheel consists of two-stage for dehumidification, two-stage for pre-cooling, and two-stage for reactivation. The results showed that the mathematical model was validated with experimental data in [3] and the operating parameters of this study are (divided desiccant wheel into six stages as illustrated above, regeneration air velocity 2.5 m s^{-1} and regeneration temperature 90 °C). Different configurations of hybrid desiccant air conditioners are presented to increase the overall performance of the system, for example, the integration of the desiccant air conditioner with a source of renewable energy such as a solar water collector [13], a solar air collector with geothermal energy [14], a solar air collector and energy storage materials [15], and solar collector [16] was used to heat the regeneration air required to reactivate the desiccant material, as a result, the energy consumption decreases and the system performance increases. Kabeel and Abdelgaied [15] studied the performance of three configurations of a hybrid system, Type A used an electric heater as a thermal source, Type B used an air solar collector and electrical air heater and Type C used an air solar collector, phase change material (PCM) and electrical air heater, the results showed that the electrical energy saving was about 20.85% and 75.82% for Type B and C as compared to Type A. Chen and Tan [16] studied the influences of incorporating chilled water from a natural cold source with the evaporative

cooler as a pre-cooling unit on the performance of a desiccant air conditioning system..

Another hybrid system can be introduced to use the highly moist air that leaves the desiccant material after the reactivation process to produce water which can be used for domestic applications, this can be done by integrating the desiccant air conditioner with a desalination unit such as humidification dehumidification unit (HDH) [17–21]. Kabeel et al., [17] studied theoretically the behavior of desiccant air conditioners incorporated with an HDH desalination unit to achieve thermal comfort conditions and produce pure drinking water. Abdelgaied et al. [18] introduced two configurations of a hybrid desiccant air conditioner integrated with an HDH desalination unit, the difference between them is that the second system utilized an additional solar collector to reheat a regeneration air before entering the desalination unit, and they found that at regeneration flow 60 m^3 h^{-1}, 120 m^3/h, 180 m^3 h^{-1}, and 240 m^3 h^{-1}, coefficient of performance varied between 0.48 and 1.11, 0.33 and 0.61, 0.23 and 0.42 and 0.18 and 0.31 and the improvement in daily yield reached 26.5%, 38.96%, 13.16%, and 11.31%, respectively. Kabeel and Abdelgaied [19] introduced a new configuration of the desiccant air conditioner to improve the quality of the supplied cooling air, and it was combined with the HDH desalination unit to produce fresh water. Wang et al. [20] improved the behavior of a hybrid desiccant air conditioner incorporated with an HDH desalination unit by utilizing the photovoltaic/thermal solar collector addition to the phase change material to satisfy the heating demands at nighttime. Saedpanah and Pasdarshahri [21] introduced solar-assisted hybrid desiccant systems with energy storage materials that are capable of providing cooling, heating, and producing fresh water suitable for remote regions.

Also, the desiccant air conditioning system can be coupled with a vapor compression cycle or absorption system when a high sensible load exists and in this case, the waste heat from the condenser can be used to heat the regeneration air required for the reactivation process [22–27]. Jani et al. [22, 23] reduced the latent part of the cooling load for vapor-compression air conditioners by incorporating the rotary desiccant dehumidifier with a vapor-compression air conditioner. They concluded that the utilization of a rotary desiccant dehumidifier reduced the humidity ratio of process air by 70% before it entered the vapor-compression air conditioner. Lee et al. [24] studied the behavior of the hybrid desiccant cooling incorporated with the electric heat pump. Hussain [25] incorporated the rotary desiccant dehumidifier with the vapor-compression air conditioner to reduce the latent part of the cooling load, and the waste heat from the condenser has been also used to reactivate the desiccant materials. Habib et al. [26] and Ali et al. [27] they integrated the absorption chiller with the solid desiccant to improve the performance of ai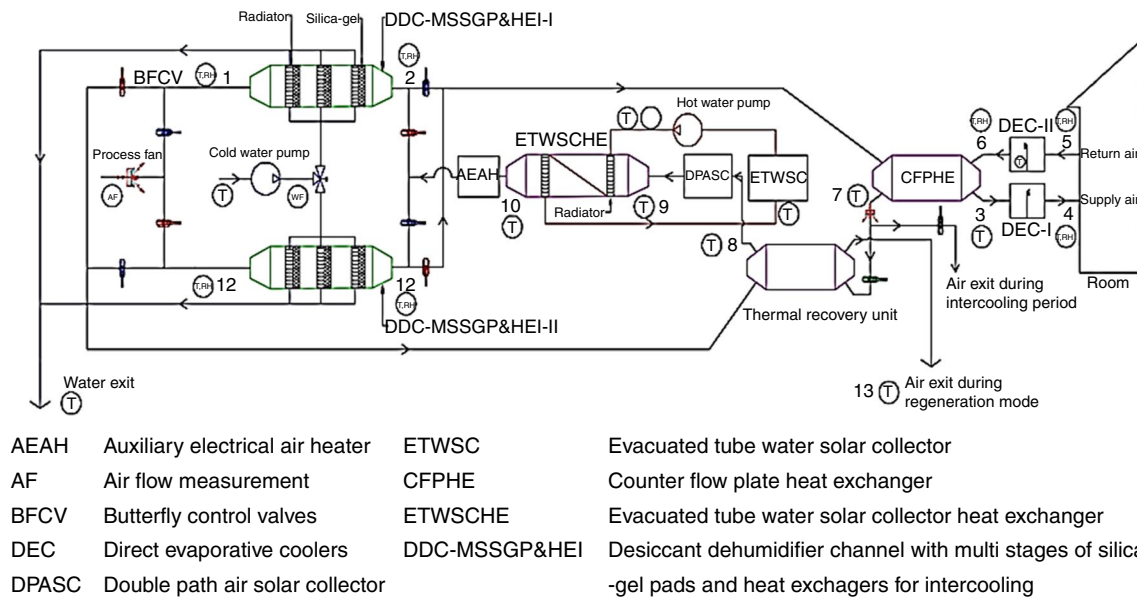r conditioner systems. They conducted that the coefficient of performance of the integrated system is 50–55% higher than the conventional solid desiccant air conditioning system.

The present experimentation work aims to design and constructed an innovative configuration of the desiccant air conditioner to achieve thermal comfort conditions for humans with the lowest rates of electrical power consumption. An innovative configuration of a desiccant dehumidifier channel with multi-stages of silica-gel pads and heat exchangers for intercooling (DDC-MSSGP&HEI) was incorporated with the air conditioner suggested in the present work to improve the quality of supplied cooling air to conditioning room, in order to achieve the thermal comfort conditions. Also, two solar collectors (Double path air solar collector and Evacuated tube water solar collector) were incorporated with the innovative configurations of the desiccant air conditioner to heat the regeneration air, adding to the auxiliary electrical heater that was utilized to set a regeneration air temperature to the required temperatures. This is in order to reduce the burden on an electricity facility and reduce environmental pollution. To achieve the lowest electrical power consumption rates, the thermal recovery unit was incorporated with the suggested desiccant air conditioner and was utilized as a preheating unit to heat the regeneration air before it enters solar collectors. The performance of the proposed innovative configuration of the desiccant air conditioner was tested under Egyptian weather conditions during the period 10:00 am to 5:00 pm.

Experimental

System description

The proposed experimental work aimed to design and constructed an innovative configuration of a desiccant air conditioner working with the lowest electrical power consumption rates and achieving thermal comfort conditions for humans. In the proposed air conditioner, to achieve thermal comfort conditions we improve the quality of cooling air supplied to the conditioning room by incorporating an innovative configuration of desiccant dehumidifier channel with multi-stages of silica-gel pads and heat exchangers for intercooling (DDC-MSSGP&HEI) with the suggest air conditioner. Also, in the proposed air conditioner to achieve the lowest electrical power consumption rates we incorporated the thermal recovery unit with the proposed hybrid system which was utilized as a preheating unit to heat the regeneration air before its inlet into the solar collectors. Figures 1 and 2 show a schematic diagram and photo of a novel configuration of the desiccant air conditioner with an innovative configuration of the desiccant dehumidifier channel and thermal recovery unit. The proposed desiccant air conditioner

Fig. 1 A schematic of an innovative configuration of a desiccant air conditioner

AEAH	Auxiliary electrical air heater	ETWSC	Evacuated tube water solar collector
AF	Air flow measurement	CFPHE	Counter flow plate heat exchanger
BFCV	Butterfly control valves	ETWSCHE	Evacuated tube water solar collector heat exchanger
DEC	Direct evaporative coolers	DDC-MSSGP&HEI	Desiccant dehumidifier channel with multi stages of silica
DPASC	Double path air solar collector		-gel pads and heat exchagers for intercooling

Fig. 2 A photographic of the proposed innovative configuration of the desiccant air conditioner
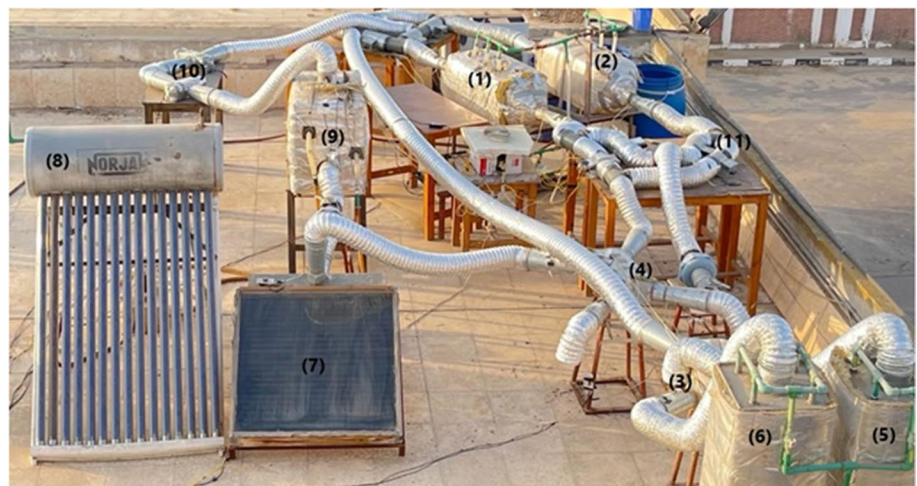
(1)	DDC-MSSGP&HEI-I	(4) Thermal recovery unit	(7) DPASC	(10) AEAH
(2)	DDC-MSSGP&HEI-II	(5) DEC-I	(8) ETWSC	(11) BFCV
(3)	CFPHE	(6) DEC-II	(9) ETWSCHE	

consists of two innovative configurations of desiccant dehumidifiers channel with multi-stages of silica-gel pads and heat exchangers for intercooling (DDC-MSSGP&HEI-I, II), counter flow plate heat exchanger (CFPHE), thermal recovery unit, two direct evaporative coolers (DEC-I, II), double path air solar collector (DPASC), evacuated tube water solar collector (ETWSC), evacuated tube water solar collector heat exchanger (ETWSCHE), auxiliary electrical air heater (AEAH), butterfly control valves (BFCV), process fan, regeneration fan, cold water pump, direct evaporative

coolers pump, and hot water pump. The description of all previous components is listed below as follows:
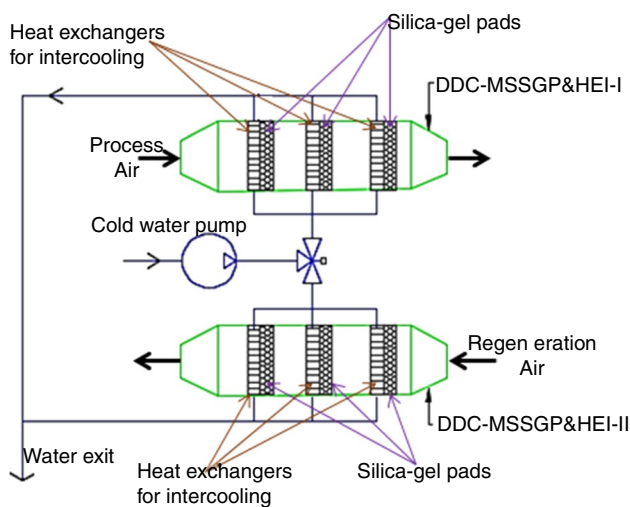
The innovative configurations of desiccant dehumidifier channel with multi-stages of silica-gel pads & heat exchangers for intercooling (DDC-MSSGP&HEI) suggested in the present work consist of the three stages of silica-gel pads that combined with three heat exchangers for intercooling. This innovative configuration of the desiccant dehumidifier channel suggested in this study was characterized by increasing the dehumidification capacity as well as cooling the process air with cooling rates higher than the heat

generated by the adsorption heat effect. So the procedure of processing air within the innovative configuration of the desiccant dehumidifier becomes dehumidification with cooling. In order to improve the quality of cooling air supplied to the conditioning room and then achieve thermal comfort conditions for humans.

This innovative configuration of desiccant dehumidifier consists of a 40 cm × 40 cm × 80 cm square channel made from 1 mm thick galvanized steel. This channel contains three stages of silica-gel pads for dehumidifying the process air; each stage is combined with a heat exchanger (radiator) for intercooling. The dimensions of each silica-gel pad are 38 cm × 35 cm × 4 cm thick. All the spaces between the channel and each stage are fully closed to prevent air leakage. The mass of silica gel is 3.83 kg for each pad and the properties of white silica gel utilized in this work are (particle size 2–5 mm, bulk density 720 kg m^{-3}, pore volume 0.35:0.45 mL g^{-1}, and surface area 650:800 m^2 g^{-1}). The dimensions of each heat exchanger (radiator) that is incorporated with the silica gel pad are 38 cm × 40 cm × 5 cm thick. The cooling water from water tanks passes through the three heat exchangers (radiators) to cool the process air and increase the ability of silica-gel to adsorb water vapor. In this proposed system, the two desiccant dehumidifier channels (DDC-MSSGP&HEI-I, II) operate at the same time but in two diverse modes (process and regeneration) as shown in Fig. 3. The outside surfaces of the two channels are insulated by (2", 48 kg m^{-3}) glass wool with a thermal conductivity coefficient of 0.041 W m^{-1}.K^{-1} to decrease the heat transfer between these two channels and their surroundings.

A counter flow plate heat exchanger (CFPHE) and thermal recovery unit contain a set of reverse parallel channels separated by thin aluminum sheets in which the process air stream and regeneration air stream flow in opposite

directions according to the counter flow principle (type GS 25). The outside surfaces of the CFPHE and thermal recovery unit are insulated by (2", 48 kg m^{-3}) glass wool with a thermal conductivity coefficient of 0.041 W m^{-1}.K^{-1} to decrease thermal heat losses.

The two direct counter flow air washer evaporative coolers (DEC-I, II) aimed to cool and humidify the air. Each one has dimensions of 40 cm × 40 cm × 105 cm height made from 1 mm thick galvanized steel and contains a cellulose gathered cooling pad as a bee-hive structure with dimensions of 40 cm × 40 cm × 40 cm. The air flows from down to up, while water is distributed over the cooling pad in opposite directions from up to down. The outside surfaces of the two DEC are insulated by (2", 48 kg m^{-3}) glass wool with a thermal conductivity coefficient of 0.041 W m^{-1}.K^{-1} to decrease the heat losses between these two DEC and their surroundings.

.To reduce the burden on the electricity facility, two solar collectors (double path air solar collector (DPASC), and evacuated tube water solar collector (ETWSC)) have been incorporated with the proposed innovative configuration of the desiccant air conditioner as shown in Fig. 2. The DPASC has dimensions of 105 cm × 100 cm × 15 cm height and contains a 2.5 m^2 surface area of v-corrugated double path copper absorber. To increase the absorption of solar energy the absorber surface was coated with black paint. The glass thickness is 3 mm and the DPASC was supported in north orientation at a constant angle of 31°. The ETWSC consists of 15 vacuum tubes 180 cm in length and a hot water tank of 100 L capacity. Two solar collectors (Double path air solar collector & Evacuated tube water solar collector) were utilized to heat the regeneration air before its entering the auxiliary electrical heater (1.5 kW) to set the regeneration air temperature at the required reactivation temperatures of the silica-gel pads using the temperature controller.

The presented experimental work contains two inline centrifugal fans one for process air and the other for regeneration air (model VKM-100, air flow rate 300 m^3 h^{-1} and fan power 60 watts). Also, it contains three pumps, each of 0.26 kW.

System operation

The proposed experimental study contains two air paths: (a) process air (supply air); (b) regeneration air (return air) as shown in Figs. 1 and 4. Consider the DDC-MSSGP&HEI-I is in process mode and the DDC-MSSGP&HEI-II is in regeneration mode. The process air is dehumidified and cooled from state 1 to state 2 in the DDC-MSSGP&HEI-I as it flows over three stages of silica-gel pads and intercooling heat exchangers. From state 2 to state 3 the process air is sensibly cooled by the return air in CFPHE. In state 3, the process air flow through DEC-I in which the process air is

Fig. 3 A schematic diagram of the DDC-MSSGP&HEI-I, II cycle
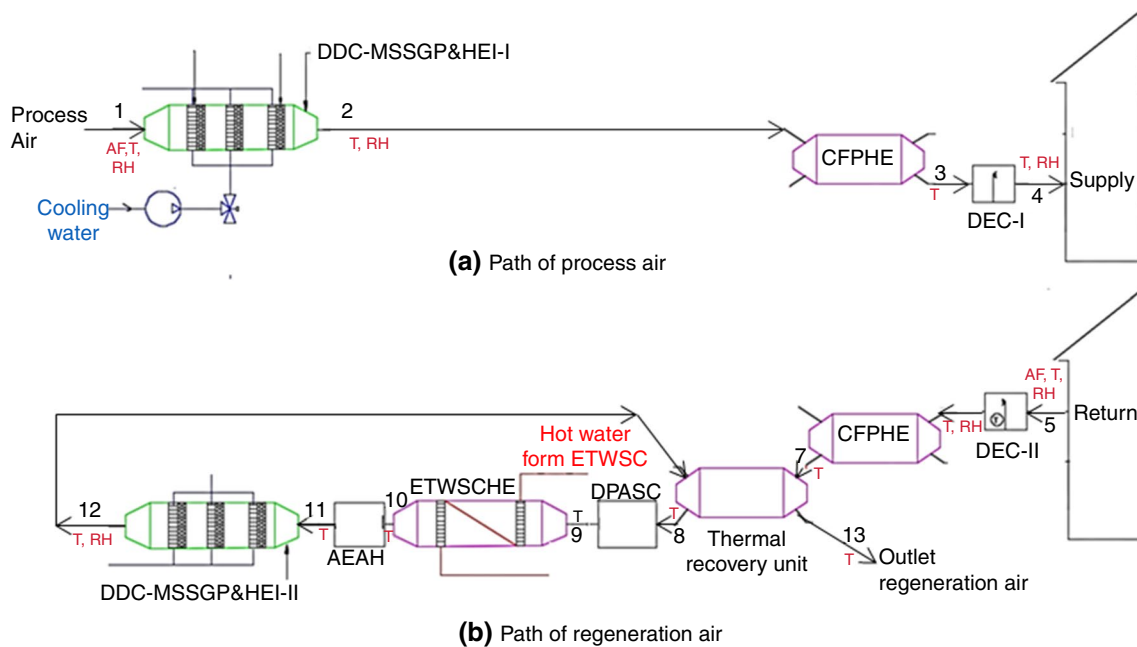
Fig. 4 A schematic diagram of the air paths of process air and regeneration air

cooled with humidified and supplied after that to the conditioning room at state 4. The amount of water that is sprayed in the DEC-I is controlled using a valve to set the supply relative humidity at 80%. Return air from the conditioning room is cooled and humidified from state 5 to state 6 in the DEC-II. From state 6 to 7 the regeneration air is sensibly heated in the CFPHE. After this, the regeneration air is sensibly heated from state 7 to state 8 in the thermal recovery unit using the thermal energy recovered from regeneration air leaving from DDC-MSSGP&HEI-II (state 12 to state 13). Also, from state 8 to state 9 and from state 9 to state 10 the regeneration air is sensibly heated in the DPASC and ETWSCHE, respectively. The AEAH is used from state 10 to state 11 to set the desired regeneration temperature which is controlled using a temperature controller. At point 11 the regeneration air enters the DDC-MSSGP&HEI-II in which a regeneration air is cooled and humidified as it flows over saturated three stages of silica-gel pads. From state 12 to state 13, regeneration air is sensibly cooled in a thermal recovery unit before being discharged into the atmosphere.

The cycle time of DDC-MSSGP&HEI-I is one hour in process mode while the cycle time of DDC-MSSGP&HEI-II is half an hour in regeneration mode and the remaining half hour of the DDC-MSSGP&HEI-II was set on cooling mode using the cooling water to cool the silica-gel pads and heat exchangers.

Cooling water is allowed to flow in the radiators of the DDC-MSSGP&HEI-I, II during process mode to decrease the process air temperature and increase the ability of silica-gel to adsorb water vapor, also during cooling mode

to decrease the DDC-MSSGP&HEI-I, II temperature then increasing the adsorption capacity in the next process mode. During cooling mode, the return air is bypassed and outlet to the atmosphere after the CFPHE, this is controlled using two BFCVs (during regeneration mode the green BFCV is open and the black BFCV is closed, and during the cooling period the green BFCV is closed and the black BFCV is open) as shown in Fig. 1. During regeneration mode, cooling water path is closed. After one hour the cycle is reversed then the DDC-MSSGP&HEI-I becomes in regeneration mode and the DDC-MSSGP&HEI-II becomes in process mode, this conversion is controlled using eight BFCV connected with Arduino Mega 2560 controller (four blue BFCV operate together and four red BFCV operate together) as shown in Fig. 1.

Instrumentation and errors analysis

To evaluate the performance of an innovative configuration of desiccant air conditioner that was suggested in a current study, the air dry bulb temperature, relative humidity, air flow rate, water temperatures, and rate of water flow were measured. The air dry bulb temperatures and relative humidity were measured using DHT22 and DS18B20 sensors. The water temperatures were measured using waterproof DS18B20 sensors. The airflow rate was calculated depending on the air velocity that was measured using the TM-401 air velocity meter. The water flow rate was measured using a water flow meter. All sensors are connected to Arduino Mega 2560 controller which is connected to the computer to

get all recorded data. The specifications and error percentages of the measuring devices are shown in Table 1. Errors in the measured data were calculated based on equations given by Coleman and Steele [28]. Thus, calculated uncertainty values are as follows: 6.5% for MRC, 5.6% for Q_c, 5.3% for DCOP, 6.4% for TCOP, and 5.1% for ECOP.

Performance evaluation indices

Dehumidification capacity DC, ($g_w\ kg_{da}^{-1}$) is defined as [29, 30]:

$$DC = \omega_{p,1} - \omega_{p,2} \tag{1}$$

Moisture removal capacity MRC, ($g_w\ s^{-1}$) is the rate of moisture removed by DDC-MSSGP&HEI which is calculated as [29, 30]:

$$MRC = \dot{m}_p\left(\omega_{p,1} - \omega_{p,2}\right) \tag{2}$$

Dehumidification coefficient of performance DCOP is a ratio of the latent heat in adsorbed moisture by DDC-MSSGP&HEI to thermal energy delivered to reactivation air which is calculated as [29, 30]:

$$DCOP = \frac{\dot{m}_p\left(\omega_{p,1} - \omega_{p,2}\right) \times h_{fg}}{\dot{Q}_{th,DPSAC} + \dot{Q}_{th,ETWSC} + \dot{Q}_{th,AEAH}} = \frac{\dot{m}_p\left(\omega_{p,1} - \omega_{p,2}\right) \times h_{fg}}{\dot{m}_{reg}C_p\left(T_{reg,11} - T_{reg,8}\right)} \tag{3}$$

Refrigeration capacity Q_c (kW) of the innovative configuration of the desiccant air conditioner is defined as:

$$\dot{Q}_c = \dot{m}_p\left(h_{p,1} - h_{p,4}\right) \tag{4}$$

Thermal coefficient of performance TCOP is a ratio between refrigeration capacity and regenerating heating capacity which is calculated as [16, 29, 30]:

$$TCOP = \frac{\dot{Q}_c}{\dot{Q}_{th,DPSAC} + \dot{Q}_{th,ETWSC} + \dot{Q}_{th,AEAH}} = \frac{\dot{m}_p\left(h_{p,1} - h_{p,4}\right)}{\dot{m}_{reg}C_p\left(T_{reg,11} - T_{reg,8}\right)} \tag{5}$$

The electrical coefficient of performance ECOP is defined as a ratio between refrigeration capacity to total electrical power consumption calculated as [29, 30]:

$$ECOP = \frac{\dot{Q}_c}{\dot{Q}_{AEAH} + P_{fans} + P_{pumps}} \tag{6}$$

Solar fraction SF is the ratio of the useful energy received by the solar collector to total thermal energy which is calculated as [29]:

$$SF = \frac{\dot{Q}_{th,DPSAC} + \dot{Q}_{th,ETWSC}}{\dot{Q}_{th,DPSAC} + \dot{Q}_{th,ETWSC} + \dot{Q}_{th,AEAH}} \tag{7}$$

Saving in the required thermal energy is defined as the ratio of the useful thermal energy recovery by the thermal recovery unit to total thermal energy which is calculated as:

$$\text{Saving in the required thermal energy} = \frac{\left(T_{reg,8} - T_{reg,7}\right)}{\left(T_{reg,11} - T_{reg,7}\right)} \tag{8}$$

Results and discussions

To illustrate the influences of innovative configurations of desiccant dehumidifier channels with multi-stages of silica-gel pads and heat exchangers for intercooling (DDC-MSSGP&HEI) and thermal recovery unit on the performance of desiccant air conditioners. The performance of a desiccant air conditioner incorporated with an innovative configuration of a desiccant dehumidifier channel and thermal recovery unit was tested under the Egyptian climate weather condition of Tanta city, Egypt within a period from 10:00 am to 5:00 pm. In the traditional rotary desiccant dehumidifier, the path of process air procedure is almost adiabatic and the air is heated by the adsorption heat effect.

Table 1 Specifications of the measuring devices

| Parameter	Sensors	Range	Accuracy	Uncertainty
Air dry bulb temperatures and relative humidity	DHT22	− 40 °C to 125 °C 0–100% RH	± 0.5 °C ± 2% RH	1.67% 3.63%
Water temperatures and air dry bulb temperatures	Waterproof DS18B20	− 55 °C to 125 °C	± 0.5 °C	1.53%
Air velocity	TM-401 air velocity meter	0.0–15 m s⁻¹	± 0.2 m s⁻¹	1.89%
Water flow rate	Water flow-meter	1.8–18 L min⁻¹	± 4%	0.65%

But, for the proposed innovative configuration of DDC-MSSGP&HEI, the combination of multi-stages of silica-gel pads with heat exchangers for intercooling is characterized by increases in the dehumidification capacity as well as cooling the process air with cooling rates higher than the heat generated by the adsorption heat effect as shown in Figs. 5 and 6. And this will be leading the path of process air procedure within DDC-MSSGP&HEI to become dehumidification with cooling.

Figure 5 shows the hourly variations of process air temperatures and humidity ratio that entering to the innovative configuration of DDC-MSSGP&HEI within the period 10:00 am to 5:00 pm for the three different test days. As shown in Fig. 1, process air temperatures entering DDC-MSSGP&HEI were varying between 32–36.5 °C, 32.6–37.8 °C, and 32.5–37.5 °C for the three test days 17 May, 18 May, and 19 May 2022, respectively. Also, the process air humidity ratio at entering DDC-MSSGP&HEI were varying between 14.5–16.3 $g_w \, kg_{da}^{-1}$, 14.6–16.2 $g_w \, kg_{da}^{-1}$, and 13.6–15.7 $g_w \, kg_{da}^{-1}$ for the three test days 17 May, 18 May, and 19 May 2022, respectively.

Figure 6 illustrates the importance of using innovative configurations of desiccant dehumidifier channels with multi-stages of silica-gel pads & heat exchangers for intercooling (DDC-MSSGP&HEI) and its influences on the temperature and humidity ratio of the process air that leaving DDC-MSSGP&HEI. It is evident from the results of the process air temperatures and humidity ratios at the outlet of DDC-MSSGP&HEI, process air temperatures at the outlet of DDC-MSSGP&HEI were decreased with rates ranging between 2.1–5.3 °C, 2.9–7.4 °C, and 3–6.8 °C for regeneration temperature 100, 90, and 80 °C, respectively as compared to process air temperature entering DDC-MSSGP&HEI. This indicates that the process air within DDC-MSSGP&HEI is cooled at cooling rates higher than the heat generated by the adsorption heat effect. These
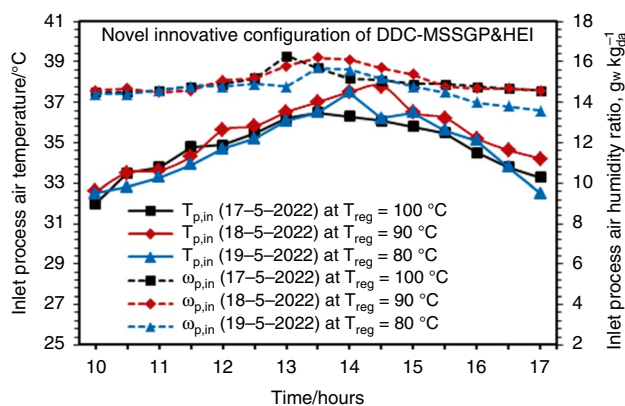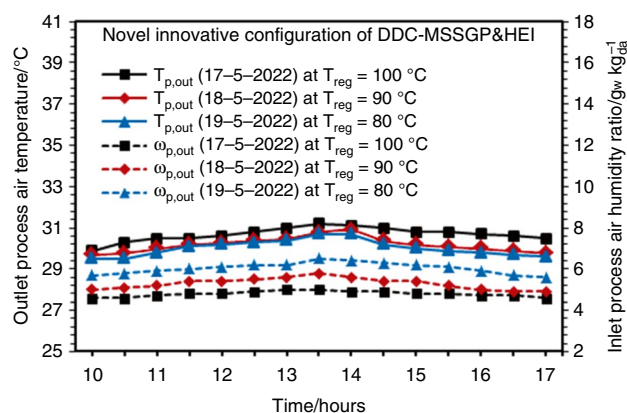
Fig. 6 Hourly variation of the process air temperatures and humidity ratio at outlet of DDC-MSSGP&HEI

will cause increases in dehumidification capacity and then reduces the humidity ratio of the process air that leaving from the DDC-MSSGP&HEI. These are mainly because of the combination of the silica-gel pads with the heat exchangers for intercooling in the innovative configurations of DDC-MSSGP&HEI. As shown in Fig. 6, process air temperatures leaving from DDC-MSSGP&HEI were varying between 29.9–31.2 °C, 29.7–30.9 °C, and 29.5–30.7 °C at regeneration temperatures 100, 90, and 80 °C, respectively. Also, the process air humidity ratio leaving from DDC-MSSGP&HEI were varying between 4.6–5 $g_w \, kg_{da}^{-1}$, 5–5.8 $g_w \, kg_{da}^{-1}$, and 5.6–6.5 $g_w \, kg_{da}^{-1}$ at regeneration temperatures 100, 90, and 80 °C, respectively.

Figures 7 and 8 show the dehumidification capacity and moisture removal capacity of the innovative configurations of DDC-MSSGP&HEI under different regeneration temperatures (100 °C, 90 °C, and 80 °C). As shown in Fig. 7, the dehumidification capacity of DDC-MSSGP&HEI ranged between 9.9–10.7 $g_w \, kg_{da}^{-1}$, 9.6–10.5 $g_w \, kg_{da}^{-1}$, and 8–9.2 $g_w \, kg_{da}^{-1}$ at regeneration temperature 100, 90, and 80 °C during the period 10:00 am-5:00 pm. Also, a moisture removal capacity was varying between 0.77–0.087 $g_w \, s^{-1}$, 0.74–0.81 $g_w \, s^{-1}$, and 0.62–0.71 $g_w \, s^{-1}$ at regeneration temperatures of 100, 90, and 80 °C during the period 10:00 am to 5:00 pm as shown in Fig. 8. The results indicated that a dehumidification capacity increases with increase regeneration temperature.

The results presented in Figs. 6–8 showed that the utilization of an innovative configuration of DDC-MSSGP&HEI represented a very effective choice, as it led to an increase in the dehumidification capacity to 10.5 $g_w \, kg_{da}^{-1}$, and the temperatures of the process air at the outlet of the DDC-MSSGP&HEI decreased at rates ranging between 2.9–7.4 °C compared to the process air temperature entering to DDC-MSSGP&HEI. This is because the process air cooling rates by the intercooler within the DDC-MSSGP&HEI were higher than the rates of heat generated by the adsorption heat
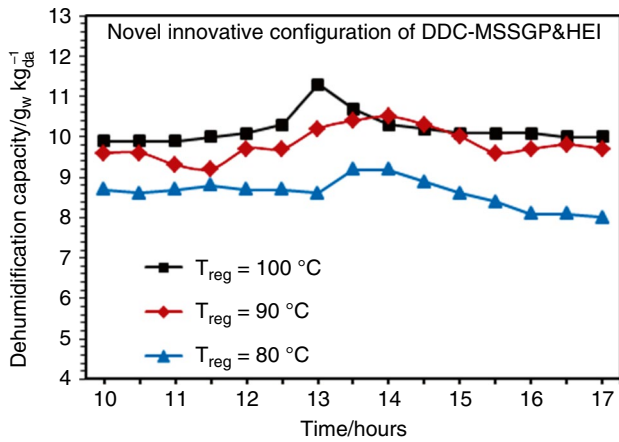

Fig. 5 Hourly variations of process air temperatures and humidity ratio entering DDC-MSSGP&HEI

Fig. 7 Hourly variations of dehumidification capacity from 10:00 am to 5;00 pm

Fig. 9 Hourly variation of the supply cooling air temperatures and humidity ratio
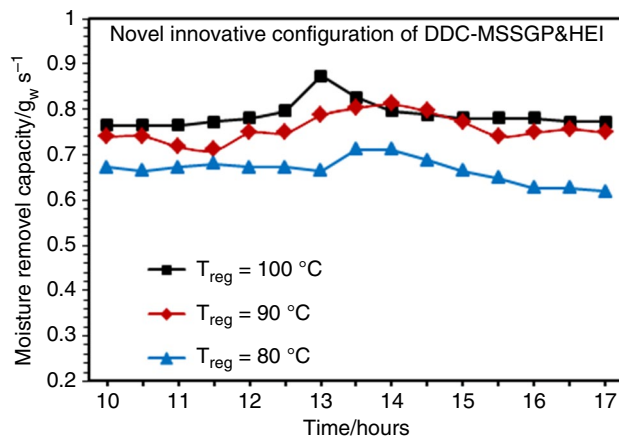

Fig. 8 Hourly variations of moisture removal capacity from 10:00 am to 5;00 pm

effect. Thus, the incorporation of multi-stages of silica-gel pads with heat exchangers for intercooling in the innovative configuration of the desiccant dehumidifier channel led to decreases in both the humidity ratio and temperature of process air leaving from DDC-MSSGP&HEI. This has been a huge challenge lately, as this helps to improve the quality of process cooling air supplied to the conditioning room and achieve thermal comfort conditions.

The influences of regeneration air temperatures on the both supply cooling air temperature and humidity ratio during the period 10:00 am-5:00 pm are presented in Fig. 9. As shown a supply cooling air temperatures varying between 12.1–12.7 °C, 12.4–13.5 °C, and 13.2–14.4 °C for regeneration temperature 100, 90, and 80 oC, respectively. These results presented that the variation in the supply cooling air temperature ranged between 1.1–1.7 °C with increases in the regeneration air temperature from 80–100 °C. This is

because the reactivation of the multi stages silica-gel pads improves with increased regeneration air temperatures. Also, the humidity ratio of the supply cooling air was varying between 7–7.3 $g_w\ kg_{da}^{-1}$, 7.2–7.7 $g_w\ kg_{da}^{-1}$, and 7.5–8.1 $g_w\ kg_{da}^{-1}$ for regeneration temperatures 100, 90, and 80 °C, respectively.

These improvements in the quality of supply cooling air are mainly due to the influence of incorporating an innovative configuration of DDC-MSSGP&HEI with the desiccant air conditioner. Where this innovative configuration of the desiccant dehumidifier will be leading the path of process air procedure to become dehumidification with cooling, and this is evident through the psychometric chart presented in Fig. 10.

Figure 10 presents the experimental data recorded for the paths of process air and regeneration air on the psychometric chart at reactivation temperatures of (a) 100 oC, (b) 90 °C, and (c) 80 °C. The process air enters the innovative configuration of the desiccant dehumidifier channel (DDC-MSSGP&HEI) at a temperature of 33.5 °C and humidity ratio of 14.5 $g_w\ kg_{da}^{-1}$ (state point-1) and exits at the temperature of 30.3 °C and humidity ratio of 4.6 $g_w\ kg_{da}^{-1}$ (state point-2) for setting the regeneration air temperature at 100 °C. While setting the regeneration temperature at 90 °C, the process air enters DDC-MSSGP&HEI at the temperature of 33.5 °C and humidity ratio of 14.7 $g_w\ kg_{da}^{-1}$ (state point-1) and exits at the temperature of 29.8 °C and humidity ratio of 5.1 $g_w\ kg_{da}^{-1}$(state point-2). But for setting the regeneration air temperature at 80 °C, the process air enters DDC-MSSGP&HEI at the temperature of 32.8 °C and humidity ratio of 14.4 $g_w\ kg_{da}^{-1}$ (state point-1) and exits at the temperature of 29.5 °C and humidity ratio of 5.8 $g_w\ kg_{da}^{-1}$ (state point-2).

It is clear from the air paths shown on the psychometric chart that the procedure inside the DDC-MSSGP&HEI (process 1–2) is dehumidification with cooling, and this
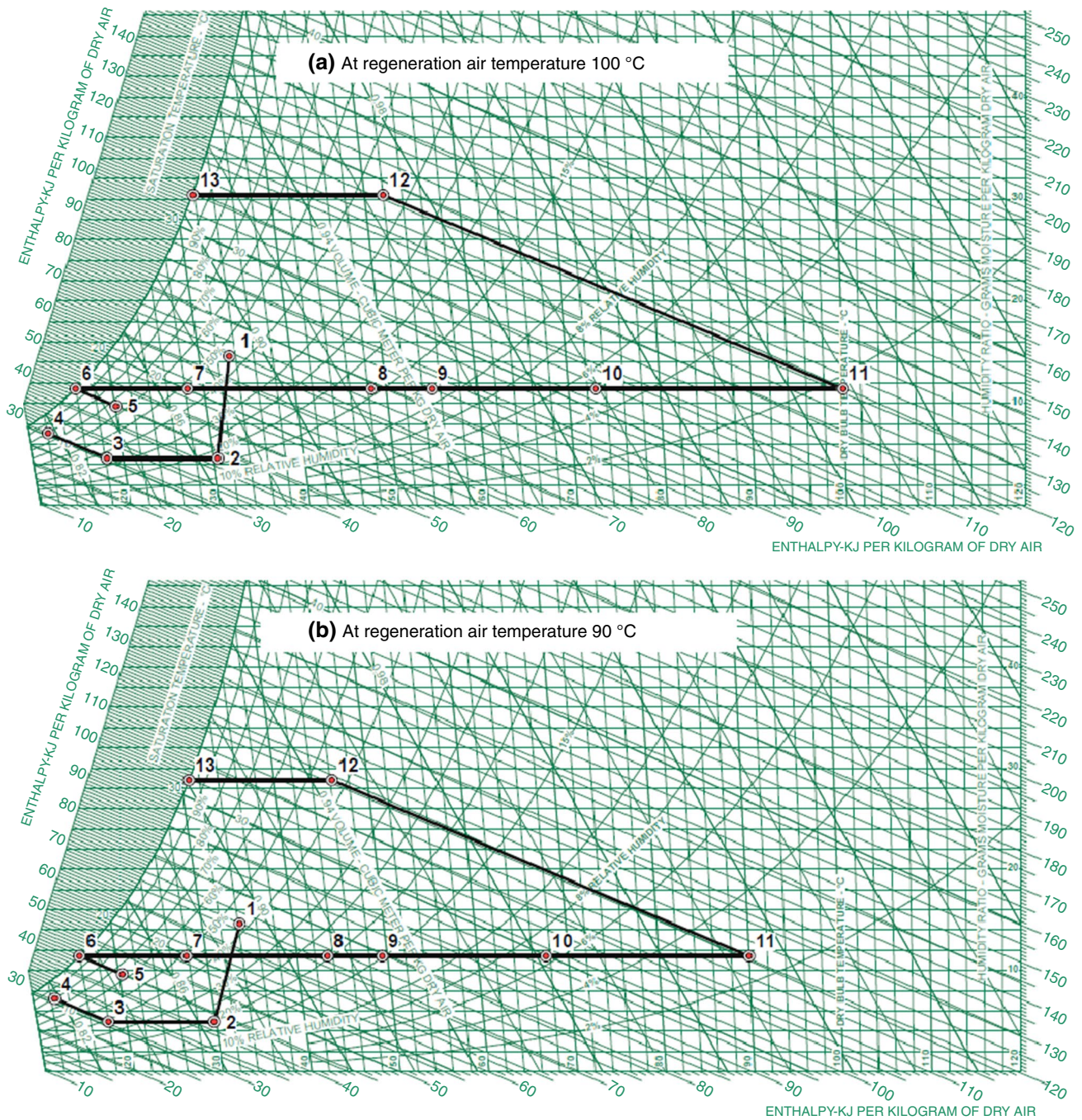
Fig. 10 Air paths on the psychometric chart at regeneration air temperatures; **a** 100 °C, **b** 90 °C, and **c** 80 °C

presented the importance of utilizing this innovative configuration of the desiccant dehumidifier channel (DDC-MSSGP&HEI) that were suggested in the present experimental work. Where, these led to improving the quality of cooling air supply to the conditioning space, as well as increasing the refrigeration capacity, and then achieving thermal comfort conditions. Where the temperatures and humidity ratio of the process air at the entrance to the conditioning space (state point-4) reached 12.1 °C & 7 g_w kg_{da}^{-1};

12.4 °C & 7.2 g_w kg_{da}^{-1}; and 13.2 °C & 7.5 g_w kg_{da}^{-1} at regeneration temperatures 100, 90, and 80 °C, respectively.

Figure 11 shows the hourly variation of refrigeration capacity of the innovative configuration of desiccant air conditioner within the period 10:00 am to 5:00 pm. As shown in this figure, the refrigeration capacity of the innovative configuration of the desiccant air conditioner was varying between 3.05–3.53 kW, 3.05–3.58 kW, and 2.63–2.93 kW for the regeneration temperatures 100, 90, and 80 °C,

(c) At regeneration air temperature 80 °C
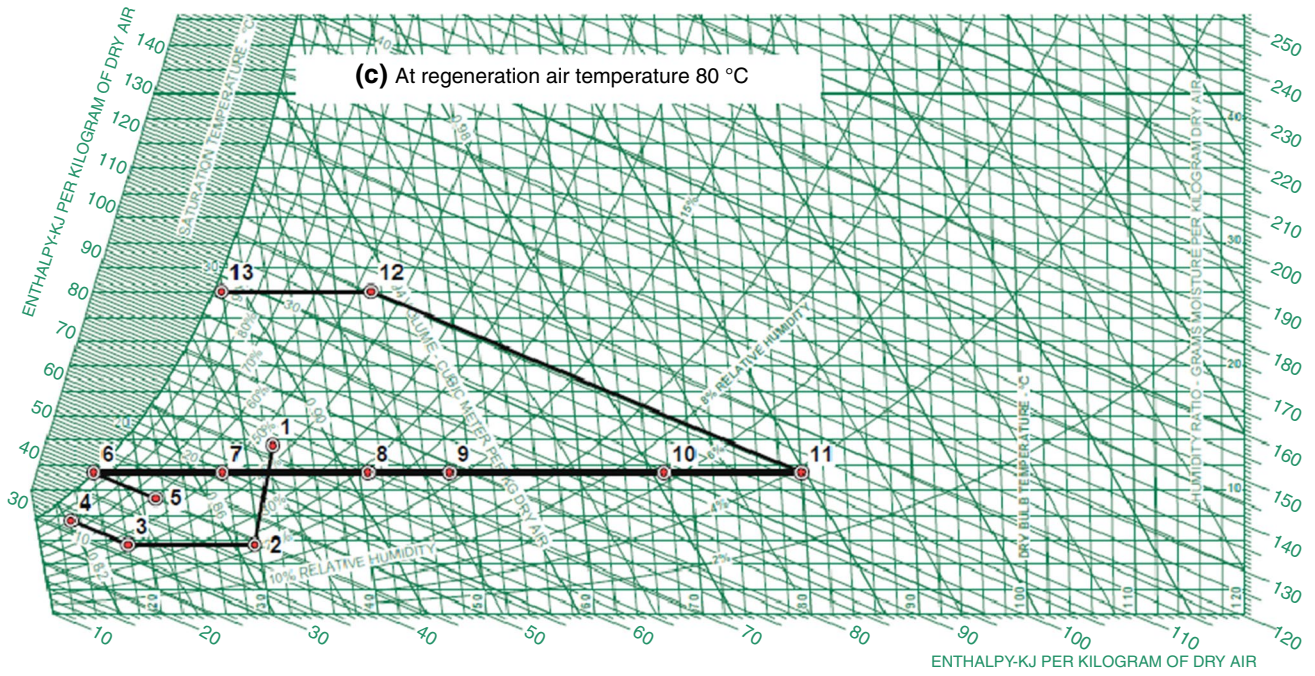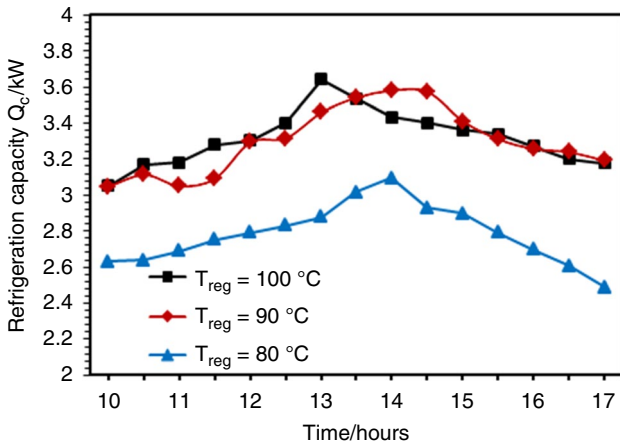
Fig. 10 (continued)

Fig. 11 Hourly variations of refrigeration capacity from 10:00 am to 5:00 pm
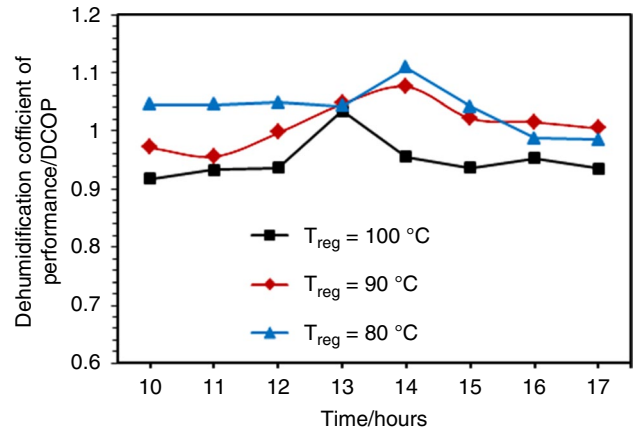

Fig. 12 Variations of dehumidification coefficient of performance (DCOP) from 10:00 am to 5:00 pm
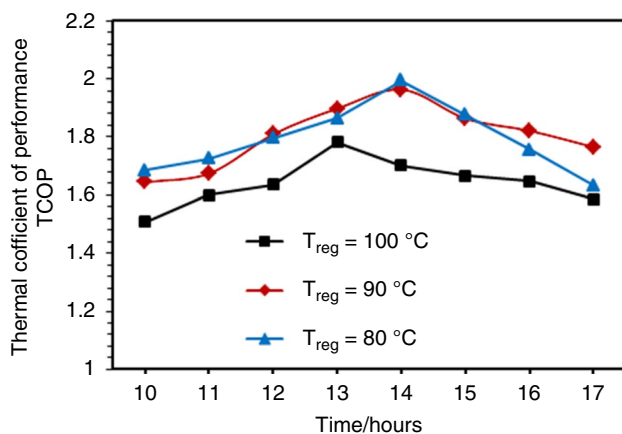
respectively within the period from 10:00 am-5:00 pm. Along the test day, the average refrigeration capacity reached 3.32 kW, 3.3 kW, and 2.78 kW for the regeneration air temperatures of 100, 90, and 80 °C, respectively. These results presented that the refrigeration capacity increase with increases in the regeneration temperatures because the dehumidification capacity of the innovative configuration of the desiccant dehumidifier channel increases with an increase in the regeneration temperatures. It was also found from the results presented in Fig. 11 that the disparity of the refrigeration capacity values at the regeneration temperature of

100 °C and 90 °C is very small, so it was recommended setting the regeneration temperature at 90 °C to achieve the highest performance with the lowest energy consumption rates.
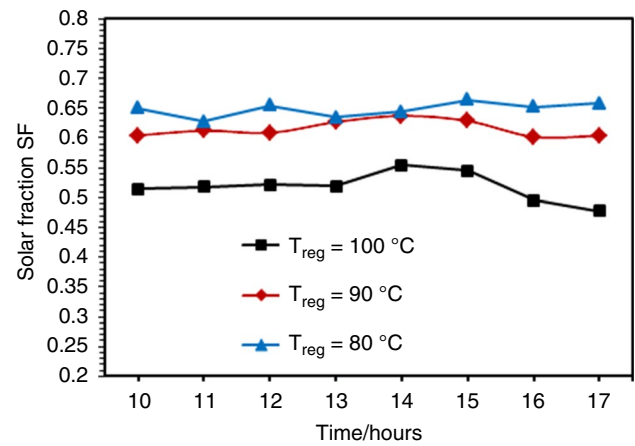
Dehumidification coefficient of performance (DCOP) plays a dynamic role in critically analyzing the performance of innovative configuration of the desiccant dehumidifier channel (DDC-MSSGP&HEI) as shown in Fig. 12. The DCOP was varying between 0.92–1.03, 0.97–1.08, and 0.98–1.11 for regeneration temperature 100, 90, and 80 °C, respectively within period 10:00 am to 5:00 pm. The average

value of DCOP reached 0.95, 1.01, and 1.04 for regeneration temperatures of 100, 90, and 80 °C, respectively. Also, the thermal coefficient of performance (TCOP) plays a dynamic role in critically analyzing the performance of an innovative configuration of the desiccant air conditioner. The TCOP represents the most important parameter to indicate the thermal performance of any system. As shown in Fig. 13, the average value of TCOP along the test day from 10:00 am-5:00 pm reached 1.64, 1.81, and 1.79 for regeneration temperatures of 100, 90, and 80 °C, respectively. These results presented that with a decrease in the regeneration temperature from 100 to 90 °C, the TCOP will be increased from 1.64 to 1.81, and this is due to the decrease in thermal energy consumption rates. But with the continued reduction in the regeneration temperature from 90 to 80 °C, the TCOP will be decreased from 1.81 to 1.79, because the reduction rates in the refrigeration capacity are higher than the saving in the consumed thermal energy. So, to achieve the highest thermal coefficient of performance (TCOP), we recommend setting the regeneration temperature at 90 °C.

In the present experimentation work, we utilized two thermal energy sources, the solar collectors (DPASC and ETWSC) represent the first thermal energy source, and an auxiliary electrical heater represents a second thermal energy source utilized to set a regeneration temperature at the required temperature. Along a test period from 10:00 am-5:00 pm, the average solar fraction reached 0.52, 0.62, and 0.65 for regeneration temperatures of 100, 90, and 80 °C, respectively as shown in Fig. 14. Use the solar collectors aimed to reduce the burden on the electricity facility, in order to reduce the environmental pollution resulting from electrical power plants that run on fossil fuels. The weather in the Middle East is characterized by being sunny almost all year round.


Fig. 14 Variations of solar fraction (SF) from 10:00 am to 5:00 pm

The heat recovery unit has also been incorporated with the innovative configuration of the desiccant air conditioner in order to save on the required thermal energy rates from the auxiliary electric air heater. The heat recovery unit was utilized as a pre-heating unit to heat the regeneration air before it enters the solar collectors and then the auxiliary electric heaters. The heat recovery unit recovers the thermal energy contained in the regeneration air that leaves from the innovative configuration of the desiccant dehumidifier channel (DDC-MSSGP&HEI) before it is expelled to the outside environment. The utilization of the thermal recovery unit causes to reduce the rate of required thermal energy from the two solar collectors (DPASC and ETWSC) and auxiliary electrical air heater from 2.685 to 1.943 kW, 2.323 to 1.758 kW, and 1.953 to 1.494 kW at regeneration temperatures of 100 °C, 90 °C, and 80 °C, respectively. As shown in Fig. 15, the average saving in the thermal energy required for regeneration air depends on the reactivation air temperature

Fig. 13 Variations of thermal coefficient of performance (TCOP) from 10:00 am to 5:00 pm
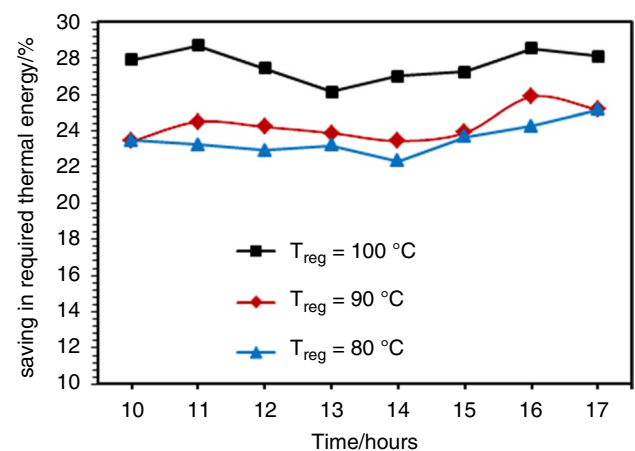
Fig. 15 Saving in required thermal energy during the period 10:00 am to 5:00 pm
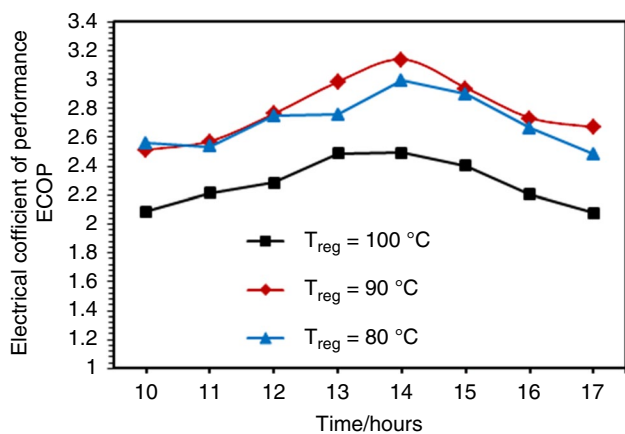
Fig. 16 Variations of electrical coefficient of performance (ECOP) from 10:00 am to 5:00 pm

which reached 27.63%, 24.3%, and 23.53% at regeneration temperatures of 100, 90, and 80 °C, respectively. These results presented that the utilization of a thermal recovery unit represents a good choice to achieve the lowest rates of electricity consumption.

Figure 16 shows the electrical coefficient of performance (ECOP) of the proposed innovative configuration of the desiccant air conditioner. As shown, the ECOP was varying between 2.08–2.49, 2.51–3.14, and 2.49–3 for regeneration temperatures of 100, 90, and 80 °C, respectively during the period from 10:00 am to 5:00 pm. The average value of the electrical coefficient of performance reached 2.28, 2.78, and 2.7 for regeneration temperatures of 100, 90, and 80 °C, respectively. So, to achieve the highest electrical coefficient of performance (ECOP), we recommend setting the regeneration temperature at 90 °C.

Economic performance

To demonstrate the economic feasibility of the proposed innovative configuration of a desiccant air conditioning system in this study, a comprehensive economic analysis was conducted for the proposed system and compared with a conventional air conditioning system for the same cooling capacity. The initial cost (IC), operating cost (OC), life cycle cost (LCC), and payback period (PP) of the proposed innovative configuration of desiccant air conditioner and the conventional air conditioning system are calculated to determine the economic feasibility of the proposed innovative system in this study. The IC is the total cost required to purchase and install the various equipment required for each system. The OC is the cost required to operate different equipment for each system and the maintenance of system equipment. LCC is the sum of IC and OC throughout the life cycle of an air conditioner system. The present value method

is used in calculating LCC, all expected future expenditures are converted to the expected present value using the present value factor (PWF) as shown in Eq. (10) [31]. The PP is the time required to recover the initial investment which is calculated using Eq. (11) [31]. It is worth noting that the system life cycle (N) is assumed to be 20 years, the interest rate (i), discount rate (d), electricity cost, and the number of working hours per year is nearly 15%, 15.7%, 0.0842 $ kWh^{-1}, and 840 h $year^{-1}$, respectively, based on projected inflation for Egypt.

$$PWF = \begin{cases} \frac{1}{d-i}\left[1 - \left(\frac{1+i}{1+d}\right)^{N}\right] If i \neq d \\ \frac{N}{1+i} If i = d \end{cases} \tag{9}$$

$$LCC = IC + (PWF \times OC) \tag{10}$$

$$PP = \frac{IC_{Proposed\ system} - IC_{reference}}{OC_{annual,\ reference} - OC_{annual,\ Proposed\ system}} \tag{11}$$

The total electricity per year, IC, OC, LCC, and PP for the proposed innovative configuration of desiccant air conditioner and conventional air conditioning system is shown in Table 2. Compared to the conventional air conditioning system, the proposed innovative configuration of desiccant air conditioner increases the IC (from 1065.8 to 1868.42$) and the annual OC decreases (from 203.7 to 65.79 $ $year^{-1}$), which results in a 33% reduction in LCC. Also, the PP of the proposed innovative configuration of the desiccant air conditioner reached 5.8 years.

Comparison with various desiccant air conditioning systems in the literature

Table 3 presents a comparison between the performances of the proposed desiccant air-conditioning system in this study with the performance of the desiccant air-conditioning systems dealt with in previous studies. This comparison aims to

Table 2 Details of IC, OC, LCC, LCS, and PP for the two air conditioning systems

	Conventional air conditioning system	Proposed innovative configuration of desiccant air conditioner
Total electricity, kWh $year^{-1}$	2419.2	781.4
IC_{total}, $	1065.8	1868.42
OC_{total}, $ $year^{-1}$	203.7	65.79
LCC, $	4391.75	2942.62
PP, year	–	5.8

Table 3 Comparison with various desiccant air conditioning systems in the literature

References	System configuration	Operating conditions	Most important results
Ge et al. [3]	Air conditioning system with one-rotor two-stage rotary desiccant cooling system	$T_{reg} = 80$ °C, process air flux 360 $m^3 h^{-1}$, and regeneration air flux 135 $m^3 h^{-1}$	TCOP equal to 0.93 ECOP equal to 0.68
Ge et al. [4]	Air conditioning with two rotary desiccant wheels	$T_{reg} = 80$ °C, process air flux 360 $m^3 h^{-1}$, and regeneration air flux 148 $m^3 h^{-1}$	TCOP equal to 0.93
Kanoğlu et al. [6]	Air conditioning with single rotary desiccant wheel	$T_{reg} = 103.9$ °C for recirculation mode and 133.4 °C for ventilation mode	TCOP equal to 1.17 for ventilation mode and 1.28 for recirculation mode
Elzahzby et al. [12]	Air conditioning system with one rotor-six stage rotary desiccant wheel and intercooling	$T_{reg} = 95$ °C, process air flux 200 $m^3 h^{-1}$, and regeneration air flux 100 $m^3 h^{-1}$	TCOP equal to 1.2 and PP equal to 6.89 years
El-Agouz and Kabeel, [14]	Air conditioning system with single rotary desiccant wheel and cooling coil unit	$T_{reg} = 90$ °C	TCOP equal to 1.03
Chen and Tan [16]	Air conditioning with single rotary desiccant wheel and natural cold source	$T_{reg} = 80$ °C	TCOP equal to 1.26
Kabeel et al. [17]	Air conditioning with single rotary desiccant wheel	$T_{reg} = 95$ °C	TCOP equal to 1.06
Kabeel and Abdelgaied, [19]	Air conditioning system with desiccant dehumidifier	$T_{reg} = 80$ °C, process air flux 120 $m^3 h^{-1}$, and regeneration air flux 120 $m^3 h^{-1}$	TCOP equal to 0.62
Wang et al. [20]	Air conditioning with single rotary desiccant wheel and Maisotsenko cycle	$T_{reg} = 83.5$ °C, process air flux 2200 $m^3 h^{-1}$, and regeneration air flux 2200 $m^3 h^{-1}$	TCOP equal to 0.41
Habib et al. [26]	Air conditioning with single rotary desiccant wheel and absorption chiller	$T_{reg} = 83$ °C and air flux 760 $m^3 h^{-1}$	TCOP equal to 1.49
Olmus et al. [29]	Air conditioning with single rotary desiccant wheel, Maisotsenko cycle, and photovoltaic/thermal water collectors	$T_{reg} = 70$ °C	TCOP equal to 0.4
Chen et al. [30]	Air conditioning with single rotary desiccant wheel and precooling unit	$T_{reg} = 106$ °C and air flux 1500 $m^3 h^{-1}$	TCOP equal to 1.2
Present experimental work	Air conditioning system with an innovative configuration of a desiccant dehumidifier channel and thermal recovery unit	$T_{reg} = 90$ °C and air flux 300 $m^3 h^{-1}$	TCOP equal to 1.96, ECOP equal to 3.14, and PP equal to 5.8 years

show the importance of utilizing the innovative configurations of a desiccant dehumidifier and thermal recovery unit in the present study and its effect on the performance of the desiccant air conditioning system. As shown in Table 3, the TCOP of the different configurations that were dealt with in previous studies ranged between 0.4 [29] and 1.49 [26], while the TCOP of the proposed air conditioning system in this study reached 1.96. It is clear from this, incorporating the proposed innovative configuration of a desiccant dehumidifier channel and thermal recovery unit with the air conditioning system represents a good choice that achieves thermal comfort conditions with the lowest electrical power consumption rates.

Conclusions

The current work aimed to design and constructed an innovative configuration of a desiccant air conditioner that achieves thermal comfort conditions for humans with the lowest electrical power consumption rates. To achieve these, the innovative configuration of DDC-MSSGP&HEI and the thermal recovery unit was incorporated with a desiccant air conditioner suggested in the present work. Also, two solar collectors (Double path air solar collector and Evacuated tube water solar collector) were incorporated with the innovative configuration of a desiccant air conditioner to heat the regeneration air, in addition to the auxiliary electrical

heater to set the regeneration air temperature to the required temperature. The performance of the proposed innovative configuration of the desiccant air conditioner was tested under Egyptian weather conditions during the period 10:00 am to 5:00 pm under three different reactivation temperatures (80 °C, 90 °C, and 100 °C). The main results follow:

- The process air within DDC-MSSGP&HEI is cooled at cooling rates higher than the heat generated by the adsorption heat effect.
- An innovative configuration of DDC-MSSGP&HEI represented a very effective choice, as it led to an increase in the dehumidification capacity to 10.5 g_w kg_{da}^{-1}, as well as the temperatures of the process air at the outlet of the DDC-MSSGP&HEI were decreased at rates ranging between 2.9–7.4 °C compared to the process air temperature entering to DDC-MSSGP&HEI.
- Incorporated the innovative configuration of DDC-MSSGP&HEI with the suggested configuration of a desiccant air conditioner that could supply the cooling air to the conditioning room with a temperature of 12.2 °C and humidity ratio of 7 g_w kg_{da}^{-1}.
- The energy performance of the innovative configuration of the desiccant air conditioner is more efficient where TCOP and ECOP reached 1.96 and 3.14, respectively at a regeneration temperature of 90 °C.
- The average saving in the required thermal energy for heating the regeneration air for utilizing the thermal recovery unit reached 27.63%, 24.3%, and 23.53% at regeneration temperatures of 100, 90, and 80 °C, respectively. These results presented that the utilization of a thermal recovery unit represents a good choice to achieve the lowest rates of electricity consumption.
- The life cycle cost (LCC) of the proposed innovative configuration of a desiccant air conditioner is 33% lower than that of the conventional air conditioning system.

References

1. Davanagere BS, Sherif SA, Goswami DY. A feasibility study of a solar desiccant air-conditioning system—part I: psychrometrics and analysis of the conditioned zone. Int J Energy Res. 1999;23:7–21.
2. Davanagere BS, Sherif SA, Goswami DY. A feasibility study of a solar desiccant air-conditioning system—part II: transient simulation and economics. Int J Energy Res. 1999;23:103–16.
3. Ge TS, Dai YJ, Wang RZ, Li Y. Experimental investigation on a one-rotor two-stage rotary desiccant cooling system. Energy. 2008;33:1807–15. https://doi.org/10.1016/J.ENERGY.2008.08.006.
4. Ge TS, Li Y, Wang RZ, Dai YJ. Experimental study on a two-stage rotary desiccant cooling system. Int J Refrig. 2009;32:498–508. https://doi.org/10.1016/J.IJREFRIG.2008.07.001.
5. Kabeel AE. Solar powered air conditioning system using rotary honeycomb desiccant wheel. Renew Energy. 2007;32:1842–57. https://doi.org/10.1016/J.RENENE.2006.08.009.
6. Kanoğlu M, Bolattürk A, Altuntop N. Effect of ambient conditions on the first and second law performance of an open desiccant cooling process. Renew Energy. 2007;32:931–46. https://doi.org/10.1016/J.RENENE.2006.04.001.
7. Henning HM, Erpenbeck T, Hindenburg C, Santamaria IS. The potential of solar energy use in desiccant cooling cycles. Int J Refrig. 2001;24:220–9. https://doi.org/10.1016/S0140-7007(00)00024-4.
8. Casas W, Schmitz G. Experiences with a gas driven, desiccant assisted air conditioning system with geothermal energy for an office building. Energy Build. 2005;37:493–501. https://doi.org/10.1016/J.ENBUILD.2004.09.011.
9. Sand JR, Fischer JC. Active desiccant integration with packaged rooftop HVAC equipment. Appl Therm Eng. 2005;25:3138–48. https://doi.org/10.1016/J.APPLTHERMALENG.2005.04.007.
10. Pennington NA. Humidity changer for air conditioning, 1955.
11. Dunkle RV. A method of solar air conditioning. Mech Chem Engnieering Trans 1965; May:73–8.
12. Elzahzby AM, Kabeel AE, Bassuoni MM, Abdelgaied M. Effect of inter-cooling on the performance and economics of a solar energy assisted hybrid air conditioning system with six stages one-rotor desiccant wheel. Energy Convers Manag. 2014;78:882–96. https://doi.org/10.1016/J.ENCONMAN.2013.06.060.
13. Bourdoukan P, Wurtz E, Joubert P. Experimental investigation of a solar desiccant cooling installation. Sol Energy. 2009;83:2059–73. https://doi.org/10.1016/J.SOLENER.2009.08.005.
14. El-Agouz SA, Kabeel AE. Performance of desiccant air conditioning system with geothermal energy under different climatic conditions. Energy Convers Manag. 2014;88:464–75. https://doi.org/10.1016/j.enconman.2014.08.027.
15. Kabeel AE, Abdelgaied M. Solar energy assisted desiccant air conditioning system with PCM as a thermal storage medium. Renew Energy. 2018;122:632–42. https://doi.org/10.1016/j.renene.2018.02.020.

16. Chen L, Tan Y. The performance of a desiccant wheel air conditioning system with high-temperature chilled water from natural cold source. Renew Energy. 2020;146:2142–57. https://doi.org/10.1016/J.RENENE.2019.08.082.

17. Kabeel AE, Abdelgaied M, Zakaria Y. Performance evaluation of a solar energy assisted hybrid desiccant air conditioner integrated with HDH desalination system. Energy Convers Manag. 2017;150:382–91. https://doi.org/10.1016/J.ENCONMAN.2017.08.032.

18. Abdelgaied M, Kabeel AE, Zakaria Y. Performance improvement of desiccant air conditioner coupled with humidification-dehumidification desalination unit using solar reheating of regeneration air. Energy Convers Manag. 2019;198:111808. https://doi.org/10.1016/J.ENCONMAN.2019.111808.

19. Kabeel AE, Abdelgaied M. A new configuration of the desiccant dehumidifier with cut-segmental silica-gel baffles and water cooling for air conditioning coupled with HDH desalination system. Int J Refrig. 2019;103:155–62. https://doi.org/10.1016/J.IJREFRIG.2019.04.009.

20. Wang N, Wang D, Dong J, Wang H, Wang R, Shao L, et al. Performance assessment of PCM-based solar energy assisted desiccant air conditioning system combined with a humidification-dehumidification desalination unit. Desalination. 2020;496:114705.

21. Saedpanah E, Pasdarshahri H. Performance assessment of hybrid desiccant air conditioning systems: a dynamic approach towards achieving optimum 3E solution across the lifespan. Energy. 2021;234:121151. https://doi.org/10.1016/J.ENERGY.2021.121151.

22. Jani DB, Mishra M, Sahoo PK. Performance studies of hybrid solid desiccant–vapor compression air-conditioning system for hot and humid climates. Energy Build. 2015;102:284–92. https://doi.org/10.1016/J.ENBUILD.2015.05.055.

23. Jani DB, Mishra M, Sahoo PK. Experimental investigation on solid desiccant–vapor compression hybrid air-conditioning system in hot and humid weather. Appl Therm Eng. 2016;104:556–64. https://doi.org/10.1016/J.APPLTHERMALENG.2016.05.104.

24. Lee Y, Park S, Kang S. Performance analysis of a solid desiccant cooling system for a residential air conditioning system. Appl Therm Eng. 2021;182:116091. https://doi.org/10.1016/J.APPLTHERMALENG.2020.116091.

25. Hussain T. Optimization and comparative performance analysis of conventional and desiccant air conditioning systems regenerated by two different modes for hot and humid climates: experimental investigation. Energy Built Environ. 2022. https://doi.org/10.1016/J.ENBENV.2022.01.003.

26. Habib MF, Ali M, Sheikh NA, Badar AW, Mehmood S. Building thermal load management through integration of solar assisted absorption and desiccant air conditioning systems: a model-based simulation-optimization approach. J Build Eng. 2020;30:101279. https://doi.org/10.1016/J.JOBE.2020.101279.

27. Ali M, Habib MF, Ahmed Sheikh N, Akhter J, Gilani SI ul H. Experimental investigation of an integrated absorption-solid desiccant air conditioning system. Appl Therm Eng 2022;203:117912. https://doi.org/10.1016/J.APPLTHERMALENG.2021.117912.

28. Coleman HW, Steele WG. Engineering application of experimental uncertainty analysis. AIAA J. 1995;33:1888–96. https://doi.org/10.2514/3.12742.

29. Olmus U¸ Güzelel YE, Pınar E, Özbek A, Büyükalaca O, Performance assessment of a desiccant air-conditioning system combined with dew-point indirect evaporative cooler and PV/T. Solar Energy 2022; 231: 566–577.

30. Chen L, Chen SH, Liu L, Zhang B. Experimental investigation of precooling desiccant-wheel air-conditioning system in a high-temperature and high-humidity environment. Int J Refrig. 2018;95:83–92.

31. Dong HW, Jeong JW. Energy and economic analysis of organic Rankine cycle for liquid desiccant system. Energy. 2022;241:122869.